Spectrochimica Acta Part B 108 (2015) 75–82

Contents lists available at ScienceDirect

Spectrochimica Acta Part B

journal homepage: www.elsevier.com/locate/sab

A multi-analytical approach to gold in Ancient Egypt: Studies on provenance and corrosion

I. Tissot [a,b,*], L.G. Troalen [c], M. Manso [a,d], M. Ponting [e], M. Radtke [f], U. Reinholz [f], M.A. Barreiros [g], I. Shaw [e], M.L. Carvalho [a], M.F. Guerra [h]

[a] LIBPhys – UNL, Faculty of Science and Technology, 2829-516 Caparica, Portugal
[b] Department of Physics, Faculty of Sciences, University of Lisbon, Campo Grande, 1649-004 Lisbon, Portugal
[c] National Museums Scotland, Collections Services Department, 242 West Granton Road, Edinburgh EH5 1JA, UK
[d] Faculdade de Belas-Artes da Universidade de Lisboa, Largo da Academia Nacional de Belas-Artes, 1249-058 Lisbon, Portugal
[e] Archaeology, Classics and Egyptology, University of Liverpool, 12-14 Abercromby Square, Liverpool L69 7WZ, UK
[f] BAM Federal Institute for Materials Research and Testing, Richard-Willstaetter-Strasse 11, 12489 Berlin, Germany
[g] LNEG, I.P., Estrada do Paço do Lumiar, 22, 1649-038 Lisbon, Portugal
[h] ArchAm, UMR 8096 CNRS - Université Paris Sorbonne, MAE, 21 allée de l'Université, 92023 Nanterre, France

ARTICLE INFO

Article history:
Received 12 December 2014
Accepted 26 March 2015
Available online 7 April 2015

Keywords:
Gold
Egypt
PGE
Provenance
Corrosion

ABSTRACT

Recent results from a three-year multi-disciplinary project on Ancient Egyptian gold jewellery revealed that items of jewellery from the Middle Kingdom to the New Kingdom were manufactured using a variety of alluvial gold alloys. These alloys cover a wide range of colours and the majority contain Platinum Group Elements inclusions. However, in all the gold foils analysed, these inclusions were found to be absent. In this work a selection of gilded wood and leather items and gold foil fragments, all from the excavations by John Garstang at Abydos (primarily from Middle Kingdom graves), were examined using Scanning Electron Microscopy-Energy Disperse Spectroscopy (SEM-EDS), X-Ray Fluorescence (μXRF), Particle Induced X-Ray Emission (μPIXE) and Double Dispersive X-Ray Fluorescence (D^2XRF). The work allowed us to characterise the composition of the base-alloys and also to reveal the presence of Pt at trace levels, confirming the use of alluvial gold deposits. Corrosion products were also investigated in the foils where surface tarnish was visually observed. Results showed that the differences in the colour of corrosion observed for the foils are related not only to the thickness of the corrosion layer but also to a multi-layer structure containing the various corrosion products.

1. Introduction

Goldwork from Ancient Egypt was made in a wide variety of colours. The few publications on the analytical study of gold and silver items show the use of a large range of gold base-alloys [1–7] and also the exploitation of gold and aurian silver sources [8,9]. One recent publication showed, however, that during the 2nd Intermediate Period (ca. 1650–1550 BC) a variety of gold colours may be observed within a single tomb and among items belonging to a single individual [5], as is also found in the New Kingdom (ca. 1550–1070 BC) [2]. This reflects the use of different alloying practices or the exploitation of gold from different origins [8].

A primary question is that of the origin of the gold. How could the Egyptian goldsmith achieve such a rich palette of gold shades? Before the introduction of parting in the metallurgical process of gold during the first millennium BC [1], diverse colours could only be achieved by the exploitation of different sources of gold.

In their publication on the excavations of Naqada and Ballas in 1896, Petrie and Quibell [10] were the first to report the presence of osmiridium inclusions in the 12th Dynasty scarab of Mu-en-ab. The presence of Platinum Group Elements (PGE) inclusions in gold is always related to the use of alluvial sources [11] and the characteristics of the PGE composition have been suggested as a possible indicator for a change of source [12].

Since the publication by Petrie and Quibell in 1896 [10], other authors have referred to the presence of PGE inclusions on the surface of Egyptian goldwork, mentioning their quite heterogeneous compositions [5,12,13]. In spite of the discovery of Os-rich and Os–Ir alloy minerals in the Eastern Desert [14], the PGE mineralogy of Egypt remains very poorly documented. Recent publications have remarked on the consistent presence of PGE inclusions on the surface of Egyptian gold jewellery [4,5,15]. With the exception of the recent analysis of gilded wood samples from the tomb of Tutankhamun, which characterised the Pt element in two regions of analysis [16], the presence of PGE inclusions in gold foils from Ancient Egypt has hitherto never been characterised.

Before the presence of PGE elements can be used to demonstrate that the foils were produced using gold from different sources (which may not be alluvial but mined), the experimental difficulties in the

* Corresponding author at: Department of Physics, Faculty of Sciences, University of Lisbon, Campo Grande, 1649-004 Lisbon, Portugal. Tel.: +351 939212005.
E-mail address: isabeltissot@gmail.com (I. Tissot).

http://dx.doi.org/10.1016/j.sab.2015.03.012
0584-8547/

identification of PGE inclusions in gold must be considered. Firstly, depending on their size, these inclusions cannot always be recognised using a stereo microscope and raking light; smaller inclusions may only be detected by increasing the magnification using Scanning Electron Microscopy (SEM). Additionally, elemental scanning using Energy Dispersive Spectroscopy (EDS) on the region of interest may be necessary.

Harris and Cabri [17] separated the PGEs into two groups: the first, less soluble in gold and usually associated with chromites, contains Ir, Os, and Ru; and the second, more soluble in gold and usually associated with sulphides, contains Rh, Pd, and Pt. For this reason, the identification of PGEs in a gold alloy is usually identified by determining the trace elements of the gold alloys (for example [18–21]). Elemental analysis of the more soluble PGEs in gold alloys is difficult to carry out because of their atomic number, as Pt and Pd are very close to the major elements of the gold alloys, respectively Au and Ag. Attempts were made to solve this problem for X-ray Fluorescence (XRF) by various approaches, using different excitation energies and data processing strategies [18,19,21].

Other question is related to the corrosion of Egyptian gold objects, which is characterised by a rose to dark purple colouration of the surface. The very thin and iridescent tarnish layer, which may in certain cases attain for gold alloys a thickness as low as 100 nm [22], has an influence on the surface appearance, and it can be misread as an intentional surface colouration. The gold tarnish phenomenon, already reported in 1926 by Lucas [23], is always attributed to the formation of silver–gold sulphides [24]. However, the influence of the gold alloy composition on the corrosion mechanism, and the identification of different corrosion products, are still not clearly understood or fully described.

In this work, as part of the multi-disciplinary CNRS funded project PICS 5995 (French National Centre for Scientific Research International Programs for scientific cooperation), and by using several analytical techniques, a selection of gilded wood and leather items and gold foil fragments, all from the excavations by John Garstang at Abydos, were investigated. These gold foils were analysed to shed more light on the composition of the gold alloys and to determine the possible presence of PGE elements. Finally, a microscopic study combined with elemental mapping was undertaken in order to identify fully the corrosion products present in the areas of the foils that were visually tarnished.

2. Archaeological context of the gold foils

Between 1906 and 1909, John Garstang, Professor of Archaeology at the University of Liverpool, undertook extensive excavations in the cemeteries at Abydos, in Upper Egypt. A detailed corpus, based on Garstang's field notes and archival data, was created by Dr Steven Snape (1987) [25]. Many of the objects from Garstang's Abydos excavations are now in the Garstang Museum of Archaeology at the University of Liverpool.

During the 1907 and 1908 seasons respectively, Garstang excavated tombs 381 and 533 at the southern edge of the so-called 'North Cemetery' at Abydos that contained gilded objects (Fig. 1a). On the basis of the other contents of these two tombs, including such diagnostic items as a decorated wooden coffin fragment in tomb 381, and an anhydrite vessel in tomb 533, both are thought to have contained the burials of Middle Kingdom individuals (ca. 2055–1650 BC).

In addition to these gilded objects, we also analysed a quantity of gold foils in the Garstang Museum that had probably originally been attached to a wooden artefact destroyed by burning (Table 1). These foils almost certainly derive from Garstang's Abydos excavations in 1908, since they are stored in the museum alongside objects clearly labelled as deriving from that season at Abydos. There is, however, no longer any indication of the date or location of the specific grave in which the foils were found (Fig. 1b).

3. Methods and instrumentation

The gold foils were analysed by complementary techniques in order to obtain information on the composition of the base-alloy, on the presence of trace elements related to PGE inclusions, and on the composition and morphology of the corrosion products present on the surface of the majority of the foils.

The elemental composition of the gold alloys was determined by using X-ray based techniques with different detection limits and spatial resolution. The base-alloys were determined by conventional SEM–EDS, XRF and Particle Induced X-ray Emission (PIXE). In addition to these, Double Dispersive X-Ray Fluorescence (D^2XRF) at the BAMline [30] at synchrotronBerliner Elektronenspeicherring-Gesellschaft für Synchrotronstrahlung (BESSY) II was used for the determination of very low concentrations of Pt in the gold alloy. Finally, the morphology of the corrosion products was observed in a Field Emission Gun - Scanning Electron Microscopy (FEG-SEM), and comparison of the compositions between corroded surfaces and un-corroded surfaces was obtained by using XRF and the EDS set-up of the FEG-SEM.

3.1. XRF

μ-XRF was carried out at LIBPhys at the New University of Lisbon with a M4 Tornado, from Bruker, (50 kV, 300 μA) comprising a Rh X-ray source with a poly-capillary lens offering a spot size down to 25 μm, coupled to a SDD detector. Spectra deconvolution was made using Bruker M-Quant software with the provided detector response function. This response function contains contributions of shelf and tail and also the enhancement of peak FWHM due to detector and electronic noise. After deconvolution the peak intensities are directly available. The accuracy of quantitative results was validated by the analysis of a set of home-made gold standards certified by other techniques [26].

3.2. PIXE

μ-PIXE was carried out at the Accélérateur Grand Louvre d'analyse élémentaire (AGLAE) accelerator of the Centre for Research and Restoration of the Museums of France (C2RMF) with a proton beam of 3 MeV, analytical spot of 50 μm diameter and SDD detectors, one covered with a Cu filter of 75 μm, at the experimental conditions specified for gold alloys [18,27]. Quantitative processing of the spectra was

Fig. 1. a) Examples of some objects from tomb 381. On the left fragments of wood with gold leaf (Liv. E. 5727) and on the right wooden object with gold leaf and black painted figures (Liv. E. 5728); b) Fragments of gold foil from Garstang's Abydos excavations in 1908 (date and tomb unknown).

Table 1
List of the objects analysed in this study with the indication of the provenance, date, description and substrate.

ID	Acc. no	Provenance	Date	Object	Substrate
1.0	4321-24	Abydos	Unknown	Wooden fragment with gold foil	–
1.1 to 1.3	4321-24	Abydos	Unknown	Gold foils	Wood
2.0	432-25	Abydos	Unknown	Wooden fragment with gold foil	–
2.1 to 2.6	432-25	Abydos	Unknown	Gold foils	Wood
3.1 to 3.5	427B E5726	Tomb 533	Middle Kingdom	Gold foils	Wood
4.1 to 4.4	E5727 Box 42	Tomb 381	Middle Kingdom	Gold foils	Leather
5.1 to 5.4	E5728 Case K	Tomb 381	Middle Kingdom	Gold foils	Wood

carried out with GUPIXWIN software [28], which was coupled to the in-house TRAUPIXE software developed at the AGLAE facility [29].

3.3. SEM–EDS

SEM–EDS at the University of Liverpool was carried out with a Jeol with a recently re-furbished ultra-thin window detector controlled by a PGT Spirit system.

SEM–EDS at NMS (National Museums Scotland) was carried out with a CamScan MX2500 coupled to a Noran Vantage EDX Si(Li) spectrometer controlled with Noran Vantage Software. Qualitative and semi-quantitative analysis of the gold foils was undertaken at the analytical working distance of 35.0 mm with 20 kV acceleration voltage, since the standard EDS spectra to perform quantitative analysis on the instrument were collected under the same standard working distance. X-ray spectra were collected in regions free of corrosion by analysing a representative area, with 300 s acquisition time. Elemental quantification was done using the ZAF matrix correction model and confirmed using a range of certified gold–silver–copper standards [4].

SEM–EDS at National Laboratory for Energy and Geology, Lisbon (LNEG), was carried out with a Philips XL 30 FEG model, with a field emission electron source operated with acceleration voltage from 10 to 15 kV. Qualitative and semi-quantitative elemental analyses were performed with an EDS microanalysis EDAX coupled to the microscope. The EDS Si(Li) detector is equipped with a 3 mm super ultra-thin window (SUTW) allowing detection of elements with low characteristic X-rays. X-ray spectra were collected in spot mode analysis for 300 s acquisition time. Semi-quantitative analyses were done by EDAX software, using ZAF matrix correction model and confirmed using a range of home-made gold standards certified by other techniques [26].

3.4. D^2XRF

In the newly developed D^2XRF the fluorescence signal is reflected under the Bragg angle from a crystal, the first energy dispersive element, towards an energy dispersive pnCCD chip [31,32]. In this way a good background reduction and an excellent energy resolution is realized with an easy mechanical set-up. In Fig. 2 the image at the Colour X-ray Camera (CXC) obtained at the energy range where the Bragg condition fulfilled is shown. For further data treatment the spectra are summed up for each row and only the intensity in the relevant energy region is processed.

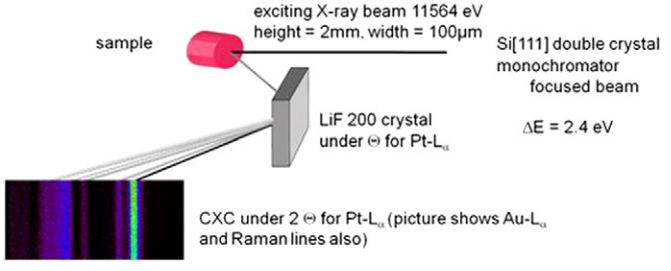

Fig. 2. Schema of the principle of the D^2XRF. The exciting monochromatic beam of 11.564 keV is producing Pt-L fluorescence in the sample. The characteristic radiation is dispersed with a LiF 200 crystal to the detector. The energy resolution of the detector allows to suppress the background efficiently and to separate the fluorescence line from the Raman scattering.

4. Results and discussion

4.1. Gold foil composition

Table 2 summarises the composition of the gold foils from Abydos characterised by SEM–EDS, PIXE and μXRF. The results obtained by SEM–EDS reflect the difficulty of elemental analysis of unprepared samples, where the analytical depth, which can be estimated at about 0.5 μm [5], is insufficient to penetrate to the core metal reflecting the elemental composition of corroded surfaces. We included in Table 2 the range of results obtained with the three EDS equipment. Nevertheless, the results show the differences between the distinct gold alloy compositions. The data show that the foils from tombs (3.1 to 5.4) have lower Ag contents compared to the foils of unknown provenance (1.0 to 2.6). Those showing more variable results for Ag are those presenting accentuated surface corrosion.

The foils were subsequently analysed by PIXE and μXRF, which have a greater penetration depth and better limits of detection than SEM–EDS. The effective penetration depth values, which represent the thickness

Table 2
Comparison of the compositional surface analysis of the fragments of gold foils investigated in this study by SEM–EDS, PIXE and μXRF. The analyses were undertaken on areas that were visually not covered with corrosion products, in order to obtain information on the base-alloys. The EDS data gives the range obtained with the 3 equipments except foils 1.0 and 2.0 (n.d = not determined).

ID	Composition in wt.%							
	SEM–EDS		PIXE			μXRF		
	Cu	Ag	Cu	Ag	Au	Cu	Ag	Au
	K_a	L_a	K_a	K_a	L_a	K_a	L_a	L_a
1.0	1	9						
1.1	0.2–0.9	1.9–3.9	0.6	3.7	95.7	0.2	3.5	96.2
1.2	0.3–0.5	1.4–4.2	0.2	3.2	96.6	n.d	2.2	97.8
1.3	0.5–0.8	1.8–5.2	0.4	5.4	94.2	0.1	5.2	94.7
2.0	2	2						
2.1	0.4–0.8	1.4–3.9	0.4	7.4	92.2	0.2	5.5	94.4
2.2	0.5–1.2	2.4–4.4	1.0	13.8	85.2	0.9	10.8	88.4
2.3	0.6–1.1	5.1–9.8	1.3	21.2	77.5	1.2	19.9	78.9
2.4	0.5–0.8	2.1–13.9				0.2	3.8	96.0
2.5	0.5–0.9	2.9–3.2	0.6	7.8	91.5	0.6	6.8	92.6
2.6						0.7	10.2	89.2
3.1	0.4–0.8	2.3–3.9	0.1	2.1	97.8	n.d	0.9	99.1
3.2	0.2–0.8	1.1–6.5	0.5	10.4	89.1	0.4	9.0	90.6
3.3	0.2–0.5	0.2–1.9	0.3	2.3	97.4	n.d	1.8	98.2
3.4	0.3–0.6	0.5–2.1	n.d	1.7	98.3	n.d	1.0	99.0
3.5	0.5–0.7	1.7–4.9	0.1	4.4	95.5	n.d	4.5	95.5
4.1	0.2–0.7	0.2–1.5	0.3	1.8	97.9	0.1	0.8	99.1
4.2	0.3–0.8	0.2–1.1	0.4	1.8	97.8	0.1	0.3	99.6
4.3	0.2–0.6	0.2–1.6				0.1	0.2	99.7
4.4	0.3–0.5	0.2–0.3				n.d	0.5	99.5
5.1	0.3–1.1	0.2–1.1				n.d	0.4	99.6
5.2	0.5–0.8	0.2–1.1	0.1	0.3	99.6	n.d	0.3	99.7
5.3	0.3–1.3	0.2–1.5				n.d	0.4	99.6
5.4	0.2–0.8	0.2–1.6				0.1	0.3	99.6

from which 95% of the detected X-rays are produced, ranges typically by PIXE between 11–16 μm for Ag(Kα) and 5–7 μm for Cu(Kα) lines depending on the composition of the gold alloy [5]. These measurements showed a generally good correlation between the compositions obtained by PIXE and μXRF.

Fig. 3 shows the ratio Ag/Au, characteristic of the source of non-refined gold, in function of the Cu contents in the alloy. The foils from tomb 381 (4.1 to 4.4 and 5.1 to 5.4) have similar compositions and are very pure, with less than 5 wt.% Ag and almost no Cu, being all the foils probably made with gold from the same source. The Ag content of some samples from the tomb 533 is higher suggesting the presence of foils with distinct compositions. The same situation can be observed for samples 1.1 to 1.3. The set of foils 2.0 to 2.6 exhibit a higher Ag content that can reach 20 wt.% and Cu contents up to 1.4 wt.%. The range of compositions obtained for the different gold foils from similar context suggests the use of gold from different provenances or the intentional use of distinct gold alloys to obtain different colours. However, neither intentional surface treatment nor higher amounts of Fe was observed for the foils.

Fig. 4 compares the Au and Ag contents obtained by μXRF for the Abydos foils with data published by Hatchfield and Newman [33] for gold leaves dated to diverse periods, with the core composition of the gold leaf from the three wood samples from the tomb of Tutankhamun published by Rifai and El Hadidi [16], and with the gilding leaf from the tomb of Qurneh published by Troalen et al. [5]. To these data we added a group of foils analysed during project PICS 5995: four gold foil specimens from the National Museums Scotland (NMS) collection dating to the 6th–18th Dynasty analysed by μXRF and a set of six gold foil specimens from the collection of the Petrie Museum of Egyptian Archaeology (PMEA) attributed to the late Middle Kingdom Harageh tomb 67, analysed with a Thermo Scientific Niton XL3t XRF analyser with GOLDD technology. If we exclude the high amount of Cu for 2 specimens of leaf published by Hatchfield and Newman [33], our data lie within the range of the few published data.

When we add to the plot the interval for primary gold samples from Egypt and Nubia published by Klemm and Klemm [34] we observe that almost all the foils from Abydos were manufactured with a higher quality alloy, out of the range of these primary gold samples. This fact could be considered as an indication of the use of alluvial gold for the production of gold foils in Abydos.

In order to explore the variety in the purity of gold within a single mining area, we also considered in this graph the data obtained for the gold grains in the quartz veins of the Um El Tuyor deposits (in the Wadi Allaqi area, at the extreme south of the Egyptian Eastern Desert) published by Zoheir [35]. Most of the gold grains are included in the interval given by Klemm and Klemm [34], however, some grains of higher purity could be detected in the laminated quartz veins. Although the published results from the mined gold include the presence of grains of higher purity fineness, the Abydos foils still lie outside the group of primary gold. Mined gold in Egypt is indeed generally expected to contain rather high Ag contents, despite a few exceptions including a few samples from the Abu Marawat mine, in the central Eastern Desert of Egypt, where visible gold/electrum and telluride specks were observed, a few reaching 98 wt.% Au [36].

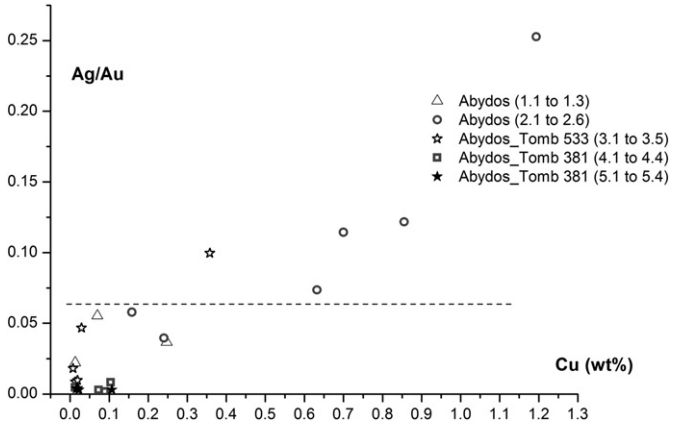

Fig. 3. Ag/Au ratio as a function of Cu (wt.%) obtained by μXRF for the gold foil fragments from tombs 381 and 533 and of unknown context from the Garstang's Abydos excavations in 1907 and 1908. The dashed line highlights the presence of one group with similar Ag/Au ratio and Cu contents suggesting the same gold source. The group is composed of foils 1.1 to 1.3, from the two tombs.

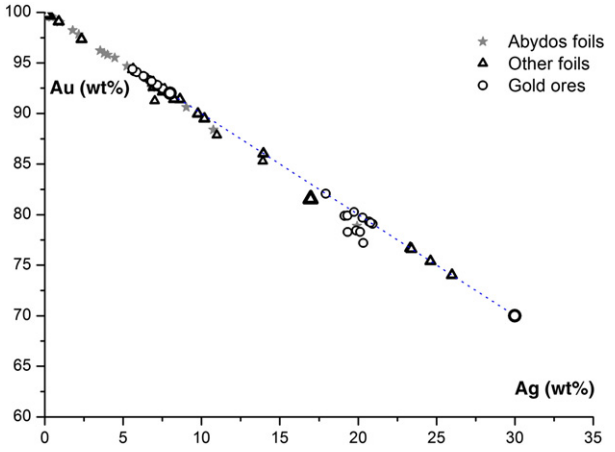

Fig. 4. Au and Ag contents for the foil specimens from Abydos compared to data obtained for a group of foils from the National Museums of Scotland and from the Petrie Museum of Egyptian Archaeology and to data published for gold leaf specimens by Hatchfield and Newman [33], Rifai and El Hadidi [16] and Troalen et al. [5] and for mined gold in Egypt and Nubia published by Klemm and Klemm [34] and by Zoheir [35].

4.2. The origin of the gold

The presence of PGE inclusions could not be identified either visually or by SEM imaging in the gold foils. However, a careful observation under the SEM FEG of a fragment of foil 2.6 showed an inclusion of quartz (Fig. 5) of about 7 μm diameter which could be linked to the use of alluvial gold. It is, however, also possible that this quartz inclusion became incorporated into the gold during metallurgical processing.

We were unable to determine the presence of any Pt in the foils by μPIXE with a minimum detection limit (MDL) of about 1000 μg/g, and because of the small size of the samples PIXE-XRF, MDL of about 80 μg/g could not be undertaken [19]. However, the recent development of a D^2XRF set-up permitted us to undertake the analysis of gold samples with a MDL as low as 1 μg/g for Pt.

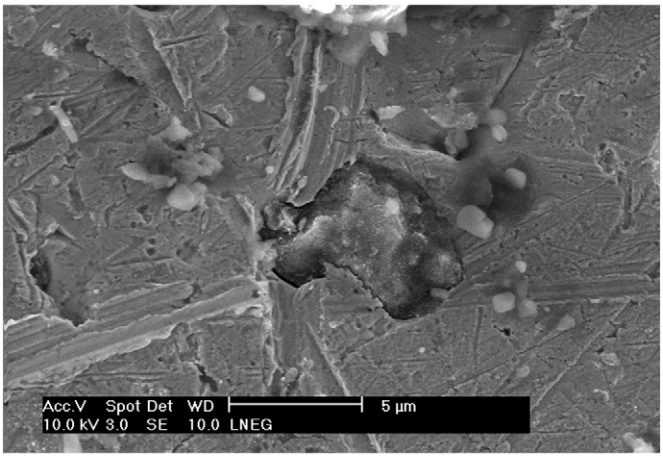

Fig. 5. SEM FEG-SE image of an inclusion of quartz on the foil Abydos 2.6 with a diameter of about 7 μm.

The concentrations of 2 fragments of foils (Abydos 2.2 and 2.3) and of a gold alloy of known composition (standard Rus: 90.3 wt.% Au, 0.3 wt.% Ag, 9.4 wt.% Cu, 200–290 μg/g Pt) determined by by Inductively coupled plasma mass spectrometry (ICP-MS) and laser ablation Inductively coupled plasma mass spectrometry (LA-ICP-MS) were calculated with the rule of proportion using gold reference material FAU8 from the Royal Canadian Mint (RCM) with 40 μg/g of Pt (Table 3). Signals were normalized prior to the calculations to the total intensity of the resonant Raman scattering [19] in the energy range from 9200 to 9350 eV. The Pt signal was summarised in the energy range from 9420 to 9460 eV prior to the calculations. The nominal energy of the Pt-Lα1 line is 9442 eV (Fig. 6). The presence of Pt could be identified and quantified in the two analysed foils at a concentration of 207–227 μg/g.

4.3. Gold foil corrosion

Eight of the gold foils from the excavations at Abydos show various degrees of tarnish. Four samples with more accentuated colour alteration were selected for further investigation using FEG-SEM–EDS and μXRF. These techniques were used in order to determine the morphology and the elemental composition of the corrosion products, according to the distinct corrosion colours.

Due to the thinness of the corrosion layer, the composition of the different corrosion colours may only be estimated. Furthermore the energy dispersive spectra of the S K-line and Au-M lines are close. For these reasons, the spectra obtained for regions with and without corrosion were compared.

Two distinct alterations of the foils were observed: i) a heterogeneous surface alteration ranging from red to blue, for example foil Abydos 2.6 (Type 1); and ii) a surface alteration characterised by a homogeneous red colouration, for example foil Abydos 2.4 (Type 2).

Type 1 corrosion corresponds typically to a bulk concentration of Ag above 9–10 wt.% and of Cu below 0.6 wt.%. Surface analysis by μXRF shows an increase of the Ag content in the corroded areas (Fig. 7). Distinct concentrations of Ag with no significant change of the S and Cu contents were obtained for each colour.

In spite of the presence of the Au-M lines close to the S-K lines, separation between gold and sulphur can be carried out because the difference between their energies is smaller than the SDD detector energy resolution (142 eV FWHM at the 5.9 keV peak of Mn). When comparing for each foil the spectra obtained in areas with and without corrosion, the spectra with corrosion show undoubtedly an enhancement at the right tail of the Au-M peaks corresponding to the S-Kα energy.

These results indicate that a relationship exists not only with the colour of the corrosion products but also with the Ag content at the surface. The increase of Ag on the corroded areas suggests the formation of an Ag-based corrosion product, which is in accordance with the results published by other authors [16,24] for some corroded gold Egyptian foils. These authors attributed the increase of Ag to the presence of distinct silver sulphide complexes, namely AgAuS and Ag_3AuS_2. It must be noted however that if Frantz and Schorsch [24] accounted for the presence of a high concentration of sulphide ions coming from the context of sealed burial chambers, Riffai and El Hadidi [16] suggested that the colouration is a possible result of an applied coating, either intentional or resulting from a modern conservation treatment.

Table 3
Concentration of Pt for the analysed standards (Fau8 and Rus) and the foils 2.2 and 2.3 from Abydos.

Sample	Counts Pt	Concentration Pt (μg/g)	Counts background	MDL Pt (μg/g)
Fau8	790	40 (Standard)	442	3.2
Rus	3123	158	907	4.6
Abydos 2.2	4483	227	1383	5.5
Abydos 2.3	4104	207	965	4.7

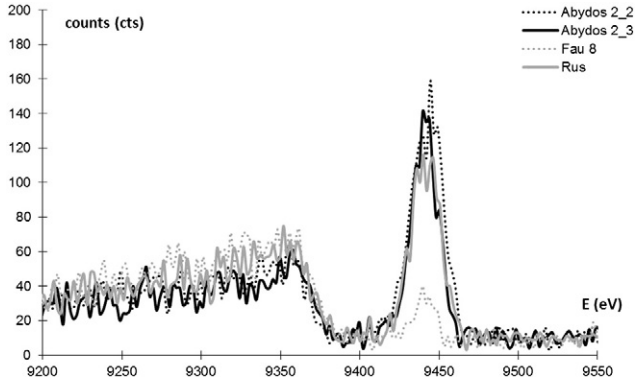

Fig. 6. Spectrum obtained by D^2XRF for Pt measurements of 2 fragments of Abydos foils and 2 standards (Fau8 and Rus).

SEM observation of the foils revealed that the morphology of the corroded surface corresponds to the presence of a corrosion product layer with a porous structure, with pore diameters of less than 100 nm (nanoporous layer), with the accentuated corrosion areas being constituted by thin and solid tubes (Fig. 8a) but morphologically different according to the distinct corrosion colour. Fig. 8b illustrates the red corrosion area constituted by a homogeneous layer and Fig. 8c shows the blue corrosion area where three distinct layers can be observed. The first layer (1) is morphologically similar to the red corrosion surface, the second layer (2) is characterised by agglomerates of corrosion products and the third layer (3) is characterised by thin tubes randomly distributed.

Considering both the compositions and the morphologies of the several corroded areas (Fig. 7), we suggest that the different colours are related not only to the thickness of the corroded layer but also to the different corrosion products, with distinct morphologies, and hence to different corrosion phases. The EDS results show an increase in the Ag content that varies according to the distinct corrosion layers (Table 4). The Ag level reaches 54 wt.% to 70 wt.% for the blue corroded area and >70 wt.% while for the red corrosion area it was only circa 17 wt.% in the base-alloy.

Corrosion of type 2 corresponds to a homogeneous corrosion, where the corroded areas revealed an accentuated increase of the S content and only a slight increase of the Ag content at the surface (Fig. 9). In this case the base alloy contains an amount of Ag of 5 wt.% and an amount of Cu below 0.3 wt.%. The corrosion layer presents an accentuated variation of S, which can be justified by the low Ag content of the base-alloy and by the strong adsorption of S on the Au alloy surface [37].

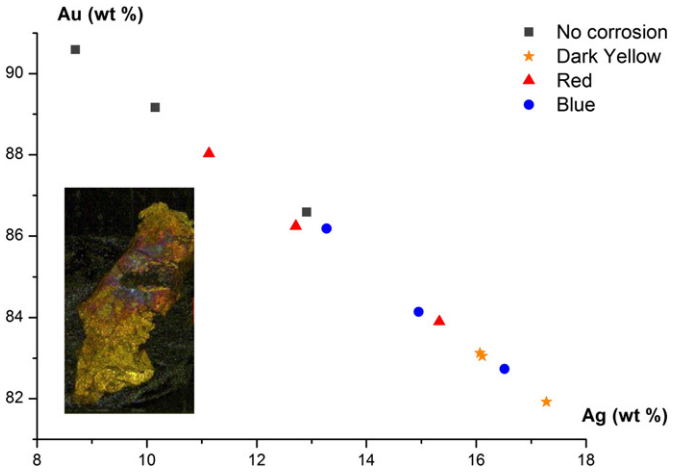

Fig. 7. Au and Ag contents obtained by μXRF for the different corrosion colours of the foil Abydos 2.6.

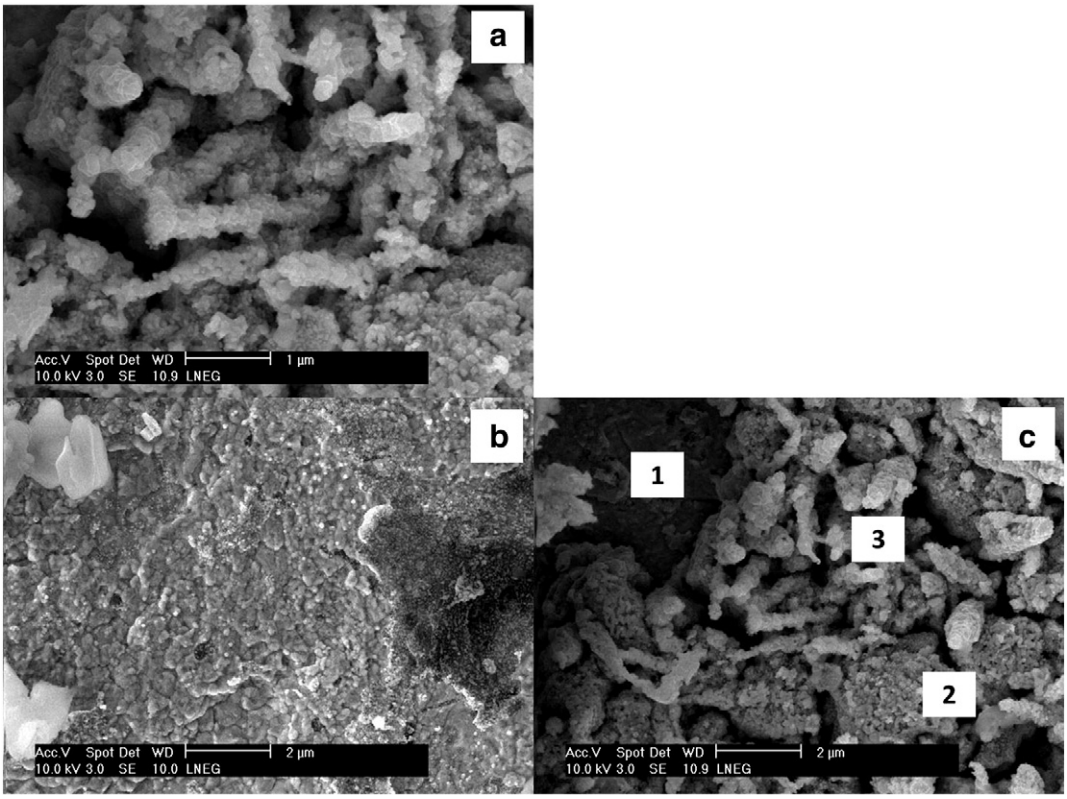

Fig. 8. SEM FEG-SE image for the heterogeneous corrosion surface (*Type 1*) on foil Abydos 2.6. a) Morphology of the corrosion products featuring very thin tubes; b) surface morphology of the red corroded area and c) of the blue area. The blue area is composed of three distinct layers: 1) one nearer the surface, morphologically similar to the red corroded areas, 2) a second with corrosion products featuring agglomerates and 3) a third with corrosion products featuring thin tubes.

The corroded surface morphology is distinct from the one of corrosion Type 1, the nanoporous layer is composed of aggregates of small round particles (Fig. 10a). The areas with more accentuated corrosion present hollow polycrystalline tubular formations randomly oriented on the top of the porous layer (Fig. 10b). The porous layer can be attributed to selective dissolution of Ag in low-Ag content Ag–Au alloys [38, 39]. The EDS analyses of the tubular formations show a homogeneous increase of the Ag contents. The area with higher concentration of tubular formation has Ag contents >20 wt.% (Fig. 10) (Table 4).

5. Conclusions

The gold foils from the Middle Kingdom objects from Garstang's tombs 381 and 533 at the southern edge of the so-called 'North Cemetery' at Abydos, and the foils that had probably originally been attached to wooden artefacts from his 1908 season excavations in Abydos, are made with different gold base alloys of distinct colours suggesting the use of gold from distinct provenances.

The high quality of the gold alloys for some specimens of leaf and foils, and the presence of a tiny quartz inclusion in one of the foils, suggest the use of alluvial gold. However, and contrary to the great majority of the few Egyptian gold work analysed until today, no PGE inclusions could so far be identified on the surface of the foils. It was only through the use of the very recently developed technique D^2XRF at BESSY II synchrotron, with a MDL ranging from 3 to 5 μg/g for the gold foils, that in this work it was possible to confirm the alluvial origin of the gold by the identification of Pt contents ranging between 207 and 227 μg/g in the analysed foils. These amounts of Pt in very thin foils

Table 4
Composition of the corrosion layer obtained by EDS compared to the base-alloy obtained by μXRF for two samples representing the two corrosion types.

			Concentration in wt.%			
		Surface	Au L_a	Ag K_a	Cu K_a	S K_a
Corrosion Type 1 (ref 2.6)						
Alloy composition		Yellow	89.2	10.2	0.7	–
Corrosion	1st layer	Red	15	80	1	4
	2nd layer	Blue	28	65	1	6
	3rd layer	Tubes	36	54	1	9
Corrosion Type 2 (ref 2.4)						
Alloy composition		Yellow	96	3.8	0.2	–
Corrosion	1st layer	Red	68	23	1	8
	2nd layer	Tubes	67	23	1	9

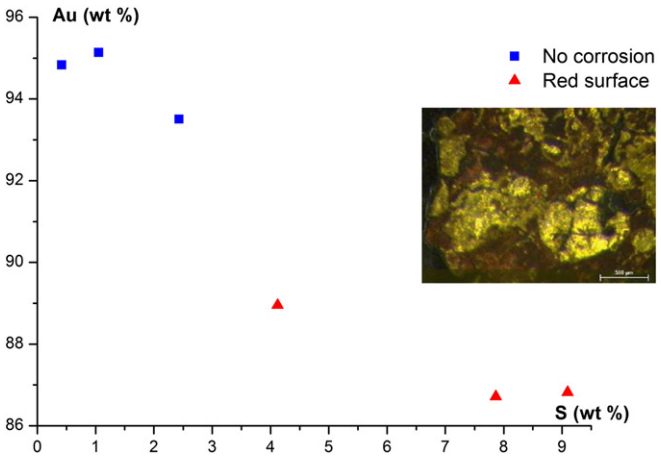

Fig. 9. Au and Ag contents obtained by μXRF for the corroded (red surface) and non-corroded areas of foil Abydos 2.4.

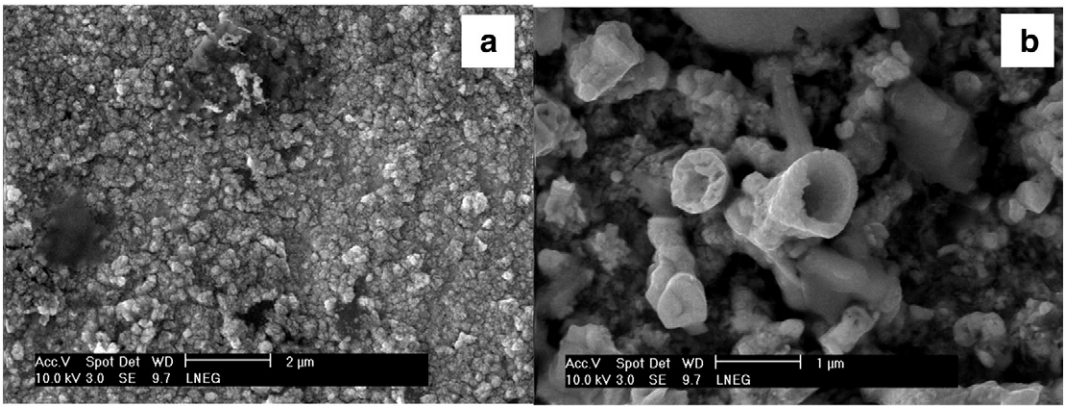

Fig. 10. SEM FEG-SE image for a) the homogeneous corrosion surface (*Type 2*) and b) a detail of the polycrystalline tubular formations of the corrosion products.

are in fact too low to be measured by any other non-destructive technique available.

Further investigation on the gold foils from the excavations at Abydos was carried out concerning the various degrees of tarnish and corrosion colours. It was possible in this work to demonstrate for the first time the presence on Egyptian corroded gold work of polycrystalline tubular formations and the occurrence of different corrosion products depending on the alloy composition and particularly on the Ag content. It was possible to relate the different Ag contents to distinct corrosion phases by showing that, according to the corrosion colour, the structure of the corrosion products is different.

Acknowledgements

We thank Gina Laycock, Dan Potter (Garstang Museum) and Ashley Cooke (Liverpool World Museum) for helping in securing additional information on the provenances and date of the gold samples from the Garstang Museum; the AGLAE team for μPIXE measurements; Jim Tate and Alison Sheridan at National Museums Scotland for the comments and suggestions while working on the manuscript.

We thank the reviewers for their comments that helped to improve the manuscript.

Financial support was provided through the Portuguese Foundation for Science and Technology (studentship to I. Tissot, grant ref. SFRH/BDE/51439/2011 and to M. Manso, grant ref. SFRH/BPD/70031/2010).

This work falls under the scope of the CNRS-funded project PICS 5995 CNRS "Analytical study of Bronze Age Egyptian gold jewellery".

References

[1] P.T. Craddock, Historical survey of gold refining. Surface treatments and refining worldwide, and in Europe prior to AD 1500, in: A. Ramage, P.T. Craddock (Eds.), King Croesus' Gold, British Museum Press, London 2000, pp. 27–53.
[2] D. Schorsch, Precious-metal polychromy in Egypt in the time of Tutankhamun, J. Egypt. Archaeol. 87 (2001) 55–71.
[3] C. Lilyquist, The Tomb of the Three Foreign Wives of Tuthmosis III, The Metropolitan Museum of Art, New York, 2003.
[4] L.G. Troalen, M.F. Guerra, J. Tate, W.P. Manley, Technological study of gold jewellery pieces dating from the Middle Kingdom to the New Kingdom in Egypt, ArchéoSciences 33 (2009) 111–119.
[5] L.G. Troalen, J. Tate, M.F. Guerra, Goldwork in ancient Egypt: workshop practices at Qurneh in the 2nd Intermediate Period, J. Archaeol. Sci. 50 (2014) 219–226.
[6] J. Ogden, Gold, in: A.J. Veldmeijer (Ed.), Tutankhamun's Footwear: Studies of Ancient Egyptian Footwear, Sidestone Press, Leiden 2011, pp. 151–164.
[7] M. Uda, S. Yoshimura, A. Ishizaki, D. Yamashita, Y. Sakuraba, Tutankhamun's golden mask investigated with XRDF, Int. J. PIXE 17 (2007) 65–76.
[8] J. Ogden, Metals, in: P.T. Nicholson, I. Shaw (Eds.), Ancient Egyptian Materials and Technologies, Cambridge University Press, Cambridge 2000, pp. 148–176.
[9] N.H. Gale, Z.A. Stos-Gale, Ancient Egyptian silver, J. Egypt. Archaeol. 67 (1981) 103–115.
[10] W.M.F. Petrie, J.E. Quibell, Naqada and Ballas, B. Quaritc, London, 1896.
[11] J. Ogden, Platinum group metal inclusions in ancient gold artefacts, Hist. Metall. 2 (1977) 53–72.
[12] N.D. Meeks, M.S. Tite, The analysis of platinum-group element inclusions in gold antiquities, J. Archaeol. Sci. 7 (1980) 267–275.
[13] J. Ogden, The so-called "platinum" inclusions in Egyptian goldwork, J. Egypt. Archaeol. 62 (1976) 138–144.
[14] A.H. Ahmed, Diversity of platinum-group minerals in podiform chromitites of the late Proterozoic ophiolite, Eastern Desert, Egypt: genetic implications, Ore Geol. Rev. 32 (2007) 1–19.
[15] G. Miniaci, S. La Niece, M.F. Guerra, M. Hacke, Analytical study of the first royal Egyptian heart-scarab, attributed to a Seventeenth Dynasty king, Sobekemsaf, Br. Mus. Tech. Res. Bull. 73 (2013) 53–60.
[16] M.M. Rifai, N.M.N. El Hadidi, Investigation and analysis of three gilded wood samples from the tomb of Tutankhamun, in: J. Dawson, C. Rozeik, M.M. Wright (Eds.), Decorated Surfaces on Ancient Egyptian Objects. Technology, Deterioration and Conservation, Archetype Publications, London 2010, pp. 16–24.
[17] D.C. Harris, L.J. Cabri, Nomenclature of platinum-group element alloys: review and revision, Can. Mineral. 29 (1991) 231–237.
[18] M.F. Guerra, Fingerprinting ancient gold with proton beams of different energy, Nucl. Instrum. Methods Phys. Res., Sect. B 226 (2004) 185–198.
[19] M.F. Guerra, M. Radtke, I. Reiche, H. Riesemeier, E. Strub, Analysis of trace elements in gold alloys by SR-XRF at high energy at the BAMline, Nucl. Instrum. Methods Phys. Res., Sect. B 266 (2008) 2334–2338.
[20] J.F. Bouchard, M.F. Guerra, Archéologie précolombienne et analyses scientifiques: la figurine d'El Angel, une œuvre composite d'orfèvrerie de la culture La Tolita-Tumaco (Équateur-Colombie), ArchéoSciences 33 (2009) 273–280.
[21] M. Radtke, I. Reiche, U. Reinholz, H. Riesemeier, M.F. Guerra, Beyond the Great Wall: gold of the Silk Roads and the first Empire of the steppes, Anal. Chem. 85 (2013) 1650–1656.
[22] D.M. Bastidas, E. Cano, A.G. González, S. Fajardo, R. Lleras-Pérez, E. Campo-Montero, F.J. Belzunce-Varela, J.M. Bastidas, An XPS study of tarnishing of a gold mask from a pre-Columbian culture, Corros. Sci. 50 (2008) 1785–1788.
[23] A. Lucas, Ancient Egyptian Materials and Industries, Edward Arnold Publishers Ltd, London, 1926.
[24] J.H. Frantz, D. Schorsch, Egyptian red gold, Archeomaterials 4 (1990) 133–152.
[25] S.R. Snape. Mortuary assemblages from Abydos, Vol. I, unpublished PhD thesis, University of Liverpool, 1987. (uk.bl.ethos.37585).
[26] I. Tissot, M. Tissot, M. Manso, L.C. Alves, M.A. Barreiros, T. Marcelo, M.L. Carvalho, V. Corregidor, M.F. Guerra, The earrings of Pancas treasure: analytical study by X-ray based techniques — a first approach, Nucl. Instrum. Methods Phys. Res., Sect. B 306 (2013) 236–240.
[27] M.F. Guerra, Role of radiation physics in the study and authentication of ancient gold work, Radiat. Phys. Chem. 95 (2014) 356–361.
[28] J.L. Campbell, N.I. Boyd, N. Grassi, P. Bonnick, J.A. Maxwell, The Guelph PIXE software package IV, Nucl. Instrum. Methods Phys. Res., Sect. B 268 (2010) 3356–3363.
[29] L. Pichon, B. Moignard, Q. Lemasson, C. Pacheco, P. Walter, Development of a multi-detector and a systematic imaging system on the AGLAE external beam, Nucl. Instrum. Methods Phys. Res., Sect. B 318 (2014) 27–31.
[30] H. Riesemeier, K. Ecker, W. Görner, B.R. Müller, M. Radtke, M. Krumrey, Layout and first XRF applications of the BAMline at BESSY II, X-Ray Spectrom. 34 (2005) 160–163.
[31] O. Scharf, S. Ihle, I. Ordavo, V. Arkadiev, A. Bjeoumikhov, S. Bjeoumikhova, G. Buzanich, R. Gubzhokov, A. Guenther, R. Hartmann, M. Kuehbacher, M. Lang, N. Langhoff, A. Liebel, M. Radtke, U. Reinholz, H. Riesemeier, H. Soltau, L. Strueder, A.F. Thuenemann, R. Wedell, Compact pnCCD-based X-ray camera with high spatial and energy resolution: a color X-ray camera, Anal. Chem. 83 (2011) 2532–2538.
[32] I. Ordavo, S. Ihle, V. Arkadiev, O. Scharf, H. Soltau, A. Bjeoumikhov, S. Bjeoumikhova, G. Buzanich, R. Gubzhokov, A. Gunther, R. Hartmann, P. Holl, N. Kimmel, M. Kuhbacher, M. Lang, N. Langhoff, A. Liebel, M. Radtke, U. Reinholz, H. Riesemeier, G. Schaller, F. Schopper, L. Struder, C. Thamm, R. Wedell, A new pnCCD-based color X-ray camera for fast spatial and energy-resolved measurements, Nucl. Instrum. Methods Phys. Res., Sect. A 654 (2011) 250–257.
[33] P. Hatchfield, R. Newman, Ancient Egyptian gilding methods, in: D. Bigelow, E. Cornu, G. Landrey, C. van Home (Eds.), Gilded Wood Conservation and History, Sound View Press, Madison CT 1991, pp. 291–299.

[34] R. Klemm, D. Klemm, Gold and Gold Mining in Ancient Egypt and Nubia. Geoarchaeology of the Ancient Gold Mining Sites in the Egyptian and Sudanese Eastern Deserts, Springer-Verlag, Berlin, 2013.
[35] B.A. Zoheir, Characteristics and genesis of shear zone-related gold mineralization in Egypt: a case study from the Um El Tuyor mine, south Eastern Desert, Ore Geol. Rev. 34 (2008) 445–470.
[36] B.A. Zoheir, A. Akawy, Genesis of the Abu Marawat gold deposit, central Eastern Desert of Egypt, J. Afr. Earth Sci. 57 (2010) 306–320.
[37] G.M. McGuirk, H. Shin, M. Caragiu, S. Ash, P.K. Bandyopadhyay, R.H. Prince, R.D. Diehl, Au(111) surface structures induced by adsorption: LEED I(E) analysis of (1×1) and (5×5) Au(111)-S phases, Surf. Sci. 610 (2013) 42–47.
[38] A. Forty, Micromorphological studies of the corrosion of gold alloys, Gold Bull. 14 (1981) 25–35.
[39] G. Hultquist, Surface enrichment of low gold alloys, Gold Bull. 18 (1985) 53–57.